

# INTERNATIONAL SOCIETY FOR SOIL MECHANICS AND GEOTECHNICAL ENGINEERING



*This paper was downloaded from the Online Library of the International Society for Soil Mechanics and Geotechnical Engineering (ISSMGE). The library is available here:*

<https://www.issmge.org/publications/online-library>

*This is an open-access database that archives thousands of papers published under the Auspices of the ISSMGE and maintained by the Innovation and Development Committee of ISSMGE.*

# Effect of hydraulic hysteresis on the consolidation of unsaturated soils

Y. Tang

*Department of Geotechnical Engineering, Nanjing Hydraulic Research Institute, Nanjing, China*

H.A. Taiebat

*Deceased, Formerly at The University of New South Wales*

A. R. Russell

*Centre for Infrastructure Engineering and Safety, School of Civil and Environmental Engineering, The University of New South Wales, Sydney, NSW, Australia*

**ABSTRACT:** Consolidation has extensive applications in geotechnical engineering practice. In this paper numerical analyses are performed to investigate the effects of hydraulic hysteresis on the one-dimensional and two-dimensional consolidation of unsaturated soils. Different initial locations of the hydraulic states on the soil-water characteristic curve (SWCC) are considered. The variations of excess pore pressures and settlement with time are presented by solving fully coupled governing equations for flow and deformation in unsaturated soils. The water and air phases are assumed to be continuous. The dependency of the coefficients of permeability and constitutive coefficients on the changes of volume and suction during the consolidation process are considered. It is shown that the different initial locations of hydraulic states result in different normalized settlements and different excess pore pressures during the consolidation of unsaturated soils.

## 1 INTRODUCTION

Consolidation is a process by which excess pore pressures dissipate and soils decrease in volume. It is an important topic in soil mechanics and has extensive applications in engineering practice, including the design of shallow foundations, embankments and other infrastructure. For example, the settlement of footings increases with time due to consolidation of the foundation soils. Being able to quantify the time dependent settlement is important since the settlement may govern the design.

Terzaghi's one-dimensional consolidation theory (Terzaghi 1943) is widely used in geotechnical engineering for the evaluation of excess water pressure and foundation settlement and is only applicable when the soil is fully saturated. For an unsaturated soil, both the excess pore air pressure and excess pore water pressure dissipate gradually with time during the consolidation process. Due to the complex interrelations between air, water and soil particles, Terzaghi's conventional consolidation theory cannot be adopted. There have been a few attempts to address the consolidation problem in unsaturated soils (e.g. Fredlund and Hasan 1979; Lloret and Alonso 1980; Dakshanamurthy et al. 1984).

Hydraulic hysteresis gives rise to non-unique relationship between suction, moisture content and void ratio of unsaturated soils. For a certain void ratio, the suction value corresponding to a moisture content depends on whether the soil has undergone a drying or wetting event to reach the current state. The hy-

draulic hysteresis influences the stress state and the mechanical behaviour of the soil (e.g. Nishimura and Fredlund 2002; Khalili and Zargarbashi 2010; Pedroso 2015). There has been no research which has addressed the effects of hydraulic hysteresis on the consolidation of unsaturated soil.

In this paper, a series of numerical analyses are performed to simulate one-dimensional (1D) and two-dimensional (2D) consolidation of unsaturated soils using a fully coupled finite element model. The hydraulic hysteresis and the dependency of the SWCC and model parameters on the volume change are considered. The effect of hydraulic hysteresis on consolidation is investigated by considering different initial locations of hydraulic states on the SWCC.

## 2 FINITE ELEMENT FORMULATION AND MODEL PARAMETERS

Khalili et al. (2008) presented the partial differential governing equations for fully coupled analysis of flow and deformation in unsaturated soil based on the effective stress principle. The finite element formulation used in this study is derived by discretizing these governing equations in domains of space and time using the Galerkin method and the implicit Euler backward interpolation scheme, respectively. The finite element formulation may be written in a matrix form as (Tang et al. 2016):

$$\begin{bmatrix} \mathbf{K} & -\psi \mathbf{L}^T & -(1-\psi) \mathbf{L}^T \\ -\psi \mathbf{L} & -a_{11} \mathbf{M} - \eta \Delta t \mathbf{H}_w & a_{12} \mathbf{M} \\ -(1-\psi) \mathbf{L} & a_{21} \mathbf{M} & -a_{22} \mathbf{M} - \eta \Delta t \mathbf{H}_a \end{bmatrix} \begin{Bmatrix} \Delta u \\ \Delta p_w \\ \Delta p_a \end{Bmatrix} = \begin{Bmatrix} \Delta \mathbf{P} \\ \Delta t \mathbf{H}_w p_w^t \\ \Delta t \mathbf{H}_a p_a^t \end{Bmatrix} + \eta \Delta t \begin{Bmatrix} \mathbf{0} \\ \mathbf{Q}_w^{t+\Delta t} \\ \mathbf{Q}_a^{t+\Delta t} \end{Bmatrix} \quad (1)$$

where  $\mathbf{K}$ ,  $\mathbf{L}$ ,  $\mathbf{H}_w$ ,  $\mathbf{H}_a$  and  $\mathbf{M}$  are the global property matrices.  $\mathbf{P}$  is the vector of nodal forces, and  $\mathbf{Q}_w$  and  $\mathbf{Q}_a$  are the vectors of nodal fluxes of the water and air flows, respectively (Tang et al. 2016).  $\Delta t$  is the increment of time over which the integration is performed.  $\eta$  is a parameter which corresponds to a particular interpolation method, with  $\eta=1$  implicit Euler backward interpolation method used in this study.  $u$ ,  $p_w$  and  $p_a$  are the nodal displacements, nodal pore water pressure and nodal pore air pressure, respectively.  $a_{11}=c_w n_w + a_{12}$ ,  $a_{12}=a_{21}=-n(\partial S_r / \partial s)$  and  $a_{22}=a_{21} + c_a n_a$  are the constitutive coefficients ensuring the coupling of air and water phases (Khalili et al. 2008).  $S_r$  is the degree of saturation.  $c_w$  and  $c_a$  are the coefficients of water and air compressibility.  $n_w$  and  $n_a$  are the volumetric water and air contents, respectively.  $n$  is the porosity of the soil.  $\psi = \partial(\chi s) / \partial s$  is the incremental effective stress parameter, in which  $s$  is the suction and  $\chi$  is the effective stress parameter.

The SWCC for a soil represents the relationship between degree of saturation and suction. The evidence that the SWCC is hysteretic has been provided through numerous laboratory studies (e.g. Poulouvasilis 1962; Topp 1969; Talsma 1970). In this study, the SWCC model proposed by Russell and Buzzi (2012) and Russell (2014) considering hydraulic hysteresis is adopted (Figure 1). The equations which link degree of saturation to suction are:

$$S_r = \begin{cases} 1 & \text{for } \frac{s}{s_e} \leq 1 \\ \left(\frac{s}{s_e}\right)^\alpha & \text{for main drying / wetting } \frac{s}{s_e} > 1 \end{cases} \quad (2-a)$$

$$S_r = \begin{cases} \left(\frac{s_{rd}}{s_{ae}}\right)^\alpha \left(\frac{s}{s_{rd}}\right)^\beta & \text{for drying reversal} \\ \left(\frac{s_{rw}}{s_{ex}}\right)^\alpha \left(\frac{s}{s_{rw}}\right)^\beta & \text{for wetting reversal} \end{cases} \quad (2-b)$$

where the pore size distribution index  $\alpha$  is the slope of the main drying and wetting curves and  $\beta$  is the slope of the scanning curves connecting the main drying and wetting curves (Russell 2014).  $s_e$  is the suction value marking the transition from unsaturated to saturated states. For the main drying curve,

$s_e = s_{ae}$  where  $s_{ae}$  is the air entry value; for the main wetting curve,  $s_e = s_{ex}$  where  $s_{ex}$  is the air expulsion value.  $s_{rd}$  and  $s_{rw}$  are the values of suction reversal on the main drying and wetting curves, respectively.

Based on the shear strength test data of different types of unsaturated soils, a definition for  $\chi$  was proposed by Khalili and Khabbaz (1998) and Khalili and Zargarbashi (2010) to include the effects of hydraulic hysteresis (Figure 1):

$$\chi = \begin{cases} 1 & \text{for } \frac{s}{s_e} \leq 1 \\ \left(\frac{s}{s_e}\right)^\Omega & \text{for main drying / wetting } \frac{s}{s_e} > 1 \end{cases} \quad (3-a)$$

$$\chi = \begin{cases} \left(\frac{s_{rd}}{s_{ae}}\right)^\Omega \left(\frac{s}{s_{rd}}\right)^\zeta & \text{for drying reversal} \\ \left(\frac{s_{rw}}{s_{ex}}\right)^\Omega \left(\frac{s}{s_{rw}}\right)^\zeta & \text{for wetting reversal} \end{cases} \quad (3-b)$$

where  $\Omega = -0.55$  is the slope of the main drying and wetting curves and  $\zeta$  is the slope of the scanning curves in a  $\ln \chi \sim \ln s$  plane (Khalili and Khabbaz 1998).

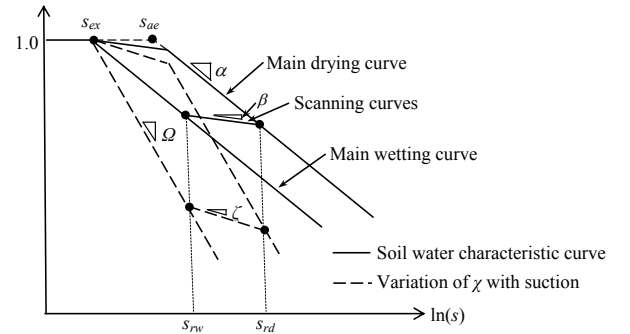


Figure 1. The soil-water characteristic curve with hydraulic hysteresis and the relationship between  $\chi$  and  $s$ .

The deformation of soil causes a change to the volume of voids and this affects the SWCC. Several models have been developed to consider the dependency of the SWCC on void ratio (e.g. Masin 2010; Salager et al. 2010; Zhou et al. 2012). The relationships which link  $S_r$  or  $\chi$  to  $s$  and volume change is captured by relating  $s_e$  to the void ratio ( $e$ ) through:

$$s_{ae} = C_2 e^{-\xi} \quad \text{and} \quad s_{ex} = C_2 e^{-\xi} / C_1 \quad (4)$$

where  $C_1$  and  $\xi$  are dimensionless constants and  $C_2$  is a constant with units of stress.

The coefficients of permeability of air phase ( $k_a$ ) and water phase ( $k_w$ ) are expressed in terms of the

intrinsic permeability ( $k$ ) and the relative permeability of air phase ( $k_{ra}$ ) and water phase ( $k_{rw}$ ) as:

$$k_a = k_{ra} \times k \text{ and } k_w = k_{rw} \times k \quad (5)$$

The relationship between intrinsic permeability and the void ratio is captured by the Kozney-Carman Equation:

$$k = \left( \frac{e^3}{1+e} \right) k_0 \left/ \left( \frac{e_0^3}{1+e_0} \right) \right. \quad (6)$$

where  $e_0$  is the reference void ratio of the soil and  $k_0$  is the reference intrinsic permeability.

The dependency of coefficients  $k_{rw}$  and  $k_{ra}$  on the suction and degree of saturation is described by the equations proposed by Brooks and Corey (1964):

$$k_{rw} = S_{eff}^{\frac{3\alpha-2}{\alpha}} \quad (7-a)$$

$$k_{ra} = (1 - S_{eff})^2 \left( 1 - S_{eff}^{\frac{\alpha-2}{\alpha}} \right) \quad (7-b)$$

where  $S_{eff} = (S_r - S_{res}) / (1 - S_{res})$  is the effective degree of saturation and  $S_{res}$  is the residual degree of saturation.

It can be found that the effective stress parameter, coefficients of permeability and constitutive coefficients are dependent on the void ratio, suction and degree of saturation of the soil and change with time during the consolidation process. At the start of consolidation, for an assumed location of the hydraulic state on the SWCC, the initial set of values of void ratio, suction, degree of saturation and other variables can be determined. The increments of nodal displacements and pore pressures over a time increment can be obtained at each time step. For the current time step the suction value is updated and the void ratio is calculated based on the volumetric strain. The SWCC is updated for the current value of void ratio and the degree of saturation can be calculated using the updated SWCC. Other variables such as the effective stress parameter, coefficients of permeability and constitutive coefficients are also calculated and updated for any subsequent time step. The nodal variables are obtained at any time step and so the solutions can be marched forward in time.

The finite element equations and the solution procedures were implemented in a general finite element program AFENA and used throughout this study.

### 3 1D AND 2D CONSOLIDATION OF UNSATURATED SOILS

The consolidation of unsaturated soils is now simulated. The surface settlement and the excess pore water and pore air pressures at every time step can be obtained. The dependency of the model parameters

on the volume and suction changes are incorporated. The effects of the hydraulic hysteresis are highlighted by assuming different initial locations of the hydraulic states on the SWCC.

Some basic assumptions are made in this paper. The water and air phases are both continuous and the soil is homogeneous. The solid skeleton and water phase are assumed incompressible. The effects of temperature change, air dissolution in water and air diffusion are neglected. The loading is assumed to be applied at  $t=0$  and maintained constant. The elastic modulus and Poisson's ratio are assumed to be constant during the consolidation process. The slight dependencies they have on the changes in suction and void ratio are ignored.

#### 3.1 1D consolidation of unsaturated soils

A single layered soil profile with a thickness of  $H=10$  m is considered and the boundary conditions are shown in Figure 2. A vertical load  $q=100$  kPa is applied to the surface of the soil. The boundary is impermeable at the bottom while the surface is free draining and allows displacement in the vertical direction. The fluids can only drain vertically from the soil surface. The details of the boundary conditions are presented in Table 1.

For a porosity  $n=0.5$ , the air entry value and air expulsion value are assumed to be 100 kPa and 50 kPa, respectively, corresponding to  $C_1=2$ . The slopes of the SWCC are assumed to be  $\alpha=-0.2$  and  $\beta=-0.1$ . The power exponent linking the air entry value to  $e$  is assumed to be  $\xi=2.7$ . The constant  $C_2=100$  kPa is also assumed. Other properties of soil include:  $k_0=1 \times 10^{-17}$  m<sup>2</sup> and  $\nu=0.25$ . The initial degree of saturation is  $S_r=0.8$ .

Table 1. Boundary conditions for 1D and 2D consolidation.

Cases	$H$ (m)	$B/D$ (m)	$q$ (kPa)	Surface	Bottom
1D	10	-	100	Free drainage	Impervious
2D Plane strain	5	2	100	Free drainage	Rough impervious

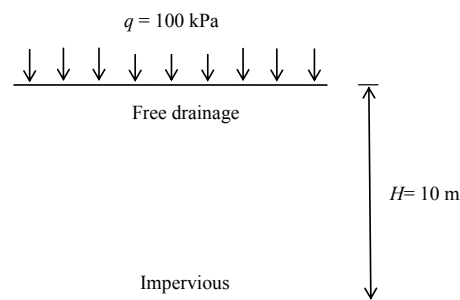


Figure 2. Boundary conditions for 1D consolidation.

The initial hydraulic states are assumed to be on a main drying curve, a main wetting curve or the mid-

point of a scanning curve. The initial suction is calculated to be 305.2kPa on the main drying curve, 152.6kPa on the main wetting curve and 215.8kPa on the scanning curve.

The elastic modulus ( $E$ ) is dependent on the soil type, stress conditions, suction and degree of saturation (Ng et al. 2009; Oh et al. 2009; Lu and Kaya 2014). Oh et al. (2009) proposed an equation which relates the elastic moduli of soils for saturated and unsaturated conditions by including the effects of suction and degree of saturation:

$$E_{unsat} = E_{sat} \left(1 + C_3 \frac{s}{(P_{atm}/100)} S_r^{C_4}\right) \quad (8)$$

where  $E_{unsat}$  and  $E_{sat}$  are the elastic moduli of the soil in unsaturated and saturated states, respectively.  $P_{atm}$  is the atmosphere pressure.  $C_3$  and  $C_4$  are fitting parameters. In this study different values of  $E$  for different initial suction values are assumed, motivated by the experimental results (e.g. Oh et al. 2009; Lu and Kaya 2014). Here the values of the saturated elastic modulus and fitting parameters are assumed to be  $E_{sat}=10$  MPa,  $C_3=1.3 \times 10^{-3}$  and  $C_4=3$ . The unsaturated elastic moduli for different initial suctions are then calculated to be:  $E_{unsat}=12$  MPa (for  $s=305.2$  kPa),  $E_{unsat}=11$  MPa (for  $s=152.6$  kPa),  $E_{unsat}=11.4$  MPa (for  $s=215.8$  kPa). The value of  $E$  has an influence on the final settlement. However, the normalized settlement is presented here and thus the value of  $E$  has no influence on the results.

Figure 3 shows the variations of normalized surface settlement and excess pore pressures with time at a depth of 5 m. Figures 3(b) and 3(c) show the variations of excess pore water and air pressures with time, respectively. The classic S-shaped curves indicate the dissipation of pore air pressure while double S-shaped curves are obtained for dissipation of excess pore water pressure. The dissipation of water pressure can be divided into two stages. During the first stage the pore air pressure diminishes completely. During the second stage the water pressure fully dissipates. Figure 3(a) shows double S-shaped curves for the variations of settlement with time. The time required to achieve the ultimate settlement is the same with that for the full dissipation of excess water pressure. There are also two stages of settlement during consolidation. The settlement in the first stage is dominated by the dissipation of both excess pore water and air pressures. The second stage is governed only by the drainage of water.

It can be seen that the different initial locations of hydraulic states result in different normalized instantaneous settlements and different initial excess pore pressures. This is very important to engineering practice because it shows that the consolidation of the soil is dependent on the hydraulic loading history, i.e. whether the soil has undergone a drying or wetting process to reach the current state.

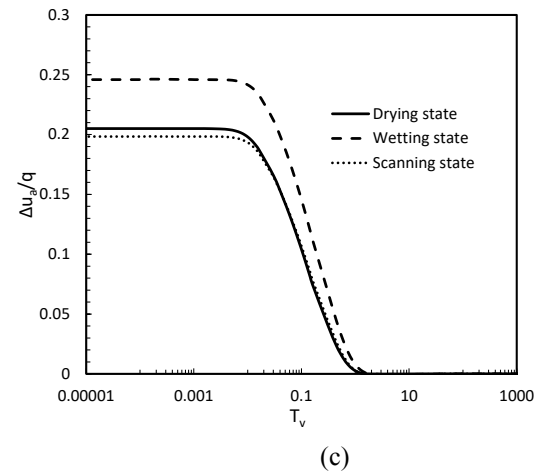
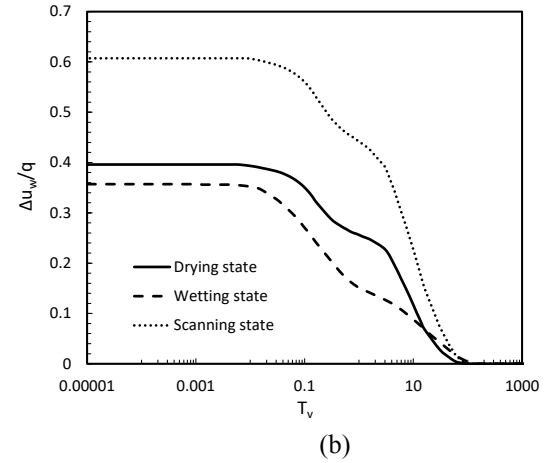
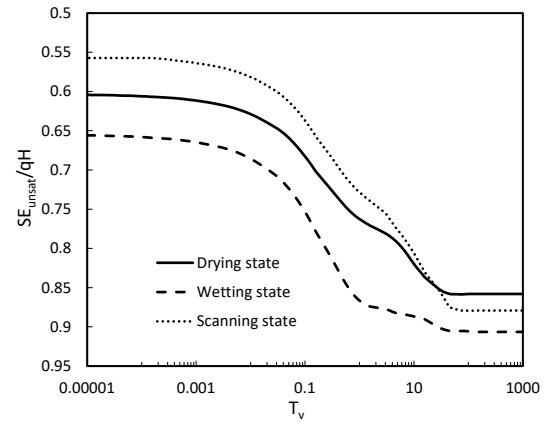


Figure 3. Numerical simulation of 1D consolidation of unsaturated soil with different initial locations of hydraulic states: (a) normalized settlement; (b) normalized excess water pressure; (c) normalized excess air pressure; versus dimensionless time factor.

The initial excess pore water pressure is largest and the instantaneous settlement and initial excess pore air pressure are smallest when the initial hydraulic state is in on the scanning curve. The reason can be attributed to the different initial values of the constitutive coefficients ( $a_{11}$ ,  $a_{12}$ ,  $a_{21}$ ,  $a_{22}$ ) which couple the deformation and the flows of water and air phases. The constitutive coefficients are dependent on the changes of  $S_r$  with respect to  $s$  on the SWCC. Figure 4 illustrates how the hydraulic states move on the SWCC during consolidation for differ-

ent initial hydraulic state locations. For the given SWCC, the initial value of  $\partial S_r / \partial s$  is largest when the initial hydraulic state is on the main wetting curve and smallest when the initial hydraulic state is on the scanning curve. It was found by Wong et al. (1998) that a larger initial excess water pressure was generated due to the applied load for a SWCC with a smaller slope. This is consistent with the results obtained here as the largest initial excess water pressure is generated when the initial hydraulic state is on the scanning curve which has the smallest slope. The locations of the final states are not the same as the initial ones although the initial and final suction values are the same since the SWCC shifts. The normalized final settlement is different due to the different increases of  $\chi s$  for the three initial locations of hydraulic states on the SWCC.

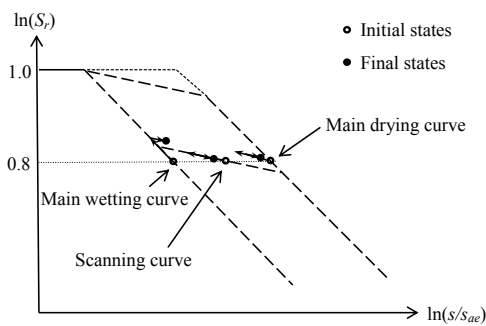


Figure 4. For a certain initial degree of saturation, illustration of how the hydraulic states move on a normalized SWCC during consolidation for different initial hydraulic state locations.

### 3.2 2D plain strain consolidation of unsaturated soils

A variety of numerical analyses are performed to simulate two-dimensional plane strain consolidation of unsaturated soils. Strip surface loadings are applied to the surface of the soil. Due to symmetry only half of the problem is modeled and the width of the domain is assumed to be equal to 6 times the half-width of the loaded area. Numerical analyses are also performed using wider meshes. There is no change to the results and thus the boundary effect can be ignored. The dependency of the model parameters, such as the permeability and the SWCC, on the changes in void ratio and suction is considered. The effects of hydraulic hysteresis are also considered. The initial values of model parameters used here are the same with 1D condition.

An unsaturated soil layer with a thickness of  $H=5$  m is subjected to a 100 kPa strip load with a width of  $B=2$  m. The bottom of the boundary is assumed to be rough and the fluids can only drain from the top boundary. The boundary conditions are shown in Figure 5. The initial hydraulic state locations are assumed to be on a main drying curve, a main wetting curve or a scanning curve. The initial degree of saturation is assumed to be 0.8.

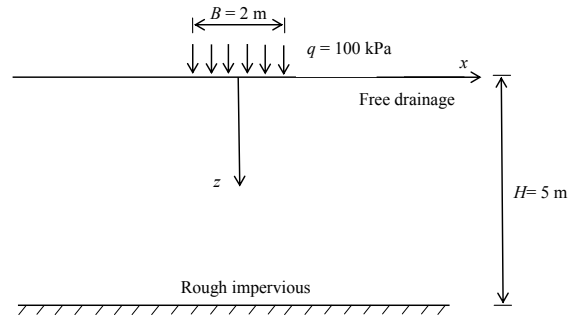


Figure 5. Boundary conditions for 2D plane strain consolidation of unsaturated soil.

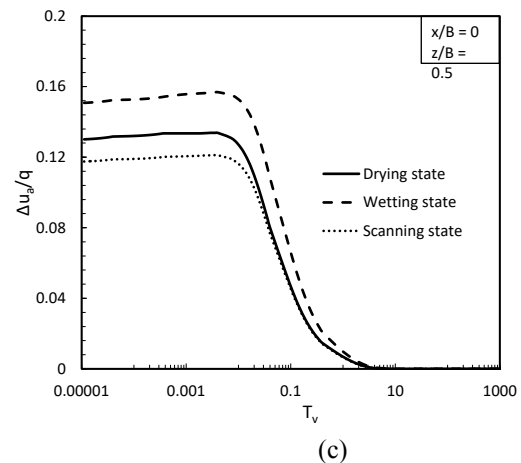
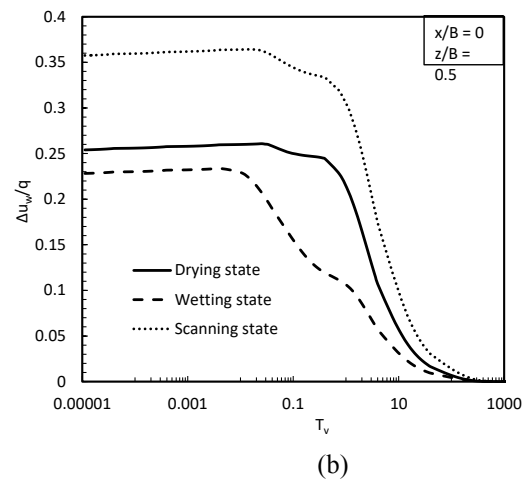
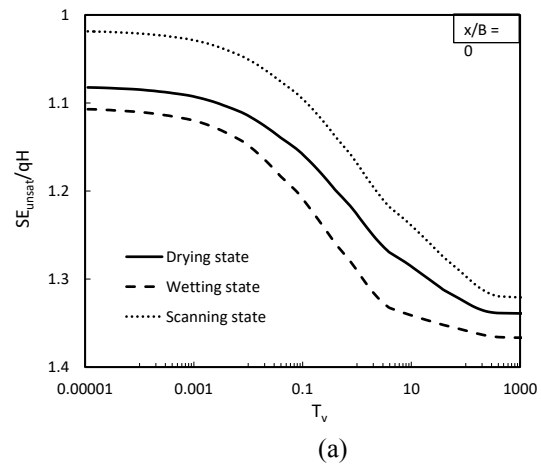


Figure 6. Numerical simulation of 2D plane strain consolidation of unsaturated soil with different initial locations of hydraulic states: (a) normalized settlement; (b) normalized excess water pressure; (c) normalized excess air pressure; versus dimensionless time factor.

Figure 6 presents the variations of normalized settlement and excess pore pressures at the depth of  $z=0.5B$  with time, respectively. Similar to the 1D condition, it can be observed that the initial locations of hydraulic states influence the 2D plane strain and axi-symmetric consolidation. For soils with a certain void ratio and degree of saturation, different initial hydraulic state locations result in different values of suction and model parameters. The immediate and final settlement and the dissipation of excess pore pressures are dependent on the hydraulic loading history.

#### 4 CONCLUSIONS

In this paper, a finite element model is adopted to simulate one-dimensional and two-dimensional consolidation of unsaturated soils. A series of analyses were performed to simulate the 1D and 2D consolidation of unsaturated soil considering the water and air phases to be continuous.

For 1D and 2D consolidation of unsaturated soil double S-shaped curves were obtained for water pressure dissipation and settlement with time. The effects of hydraulic hysteresis on the consolidation of unsaturated soil were studied. For soils with the same void ratio and degree of saturation, different initial locations of hydraulic states on the SWCC resulted in different settlements and excess pore pressures. The hydraulic loading history of the soil should be considered when assessing the settlement.

#### REFERENCES

- AFENA [Computer software]. University of Sydney, Sydney, Australia.
- Brooks, R.H. & Corey, A.T. 1964. Hydraulic properties of porous medium. *Hydrology Paper 3*, Colorado State University, Fort Collins, CO.
- Dakshanamurthy, V., Fredlund, D.G. & Rahardjo, H. 1984. Coupled three-dimensional consolidation theory of unsaturated porous media. *Proc., 5th Int. Conf. on Expansive Soils*, Adelaide, Australia, 99-103.
- Fredlund, D.G. & Hasan, J.U. 1979. One-dimensional consolidation theory: unsaturated soils. *Canadian Geotechnical Journal* 17(3): 521-531.
- Khalili, N., Habte, M., & Zargargashi, S. 2008. A fully coupled flow deformation model for cyclic analysis of unsaturated soils including hydraulic and mechanical hysteresis. *Computers and Geotechnics* 35(6), 872-889.
- Khalili, N. & Khabbaz, M.H. 1998. A unique relationship for the determination of the shear strength of unsaturated soils. *Géotechnique* 48(5): 681-687.
- Khalili, N. & Zargarbashi, S. 2010. Influence of hydraulic hysteresis on effective stress in unsaturated soils. *Géotechnique* 60: 729-734.
- Lloret, A. & Alonso, E.E. 1980. Consolidation of unsaturated soils including swelling and collapse behaviour. *Géotechnique* 30: 449-477.
- Lu, N. & Kaya, M. 2014. Power law for elastic moduli of unsaturated soil. *Journal of Geotechnical and Geoenvironmental Engineering* 140(1): 46-56.
- Masin, D. 2010. Predicting the dependency of a degree of saturation on void ratio and suction using effective stress principle for unsaturated soils. *International Journal for Numerical and Analytical Methods in Geomechanics* 34(1): 73-90.
- Ng, C.W.W., Xu, J. & Yung, S.Y. 2009. Effects of imbibition drainage and stress ratio on anisotropic stiffness of an unsaturated soil at very small strains. *Canadian Geotechnical Journal* 46(9): 1062-1076.
- Nishimura, T., & Fredlund, D.G. 2002. Hysteresis effects resulting from drying and wetting under relatively dry conditions. *Proc., 3rd Int. Conf. on Unsaturated Soils*, Swets and Zeitlinger, Lisse, 301-305.
- Oh, W.T., Vanapalli, S.K. & Puppala, A.J. 2009. Semi-empirical model for the prediction of modulus of elasticity for unsaturated soils. *Canadian Geotechnical Journal* 46: 903-914.
- Pedroso, D.M. 2015. A consistent u-p formulation for porous media with hysteresis. *International Journal for Numerical Methods in Engineering* 101, 606-634.
- Poulovassilis, A. 1962. Hysteresis of pore water-an application of the concept of independent domains. *Soil Science* 92: 405-412.
- Qin, A.F., Chen, G.J., Tan, Y.W. & Sun, D.A. 2008. Analytical solution to one-dimensional consolidation in unsaturated soils. *Applied Mathematics and Mechanics* 29(10): 1329-1340.
- Russell, A.R. 2014. How water retention in fractal soils depends on particle and pore sizes, shapes, volumes and surface areas. *Géotechnique* 64(5): 379-390.
- Russell, A.R. & Buzzi, O. 2012. A fractal basis for soil-water characteristics curves with hydraulic hysteresis. *Géotechnique* 62(3): 269-274.
- Salager, S., El Youssoufi, M.S. & Saix, C. 2010. Definition and experimental determination of a soil-water retention surface. *Canadian Geotechnical Journal* 47(6): 609-622.
- Talsma, T. 1970. Hysteresis in two sands and the independent domain model. *Water Resources Research* 6: 964-970.
- Tang, Y., Taiebat, H. & Russell, A.R. 2016. Bearing capacity of shallow foundations in unsaturated soil considering hydraulic hysteresis and three drainage conditions. *International Journal of Geomechanics*, DOI: 10.1061/(ASCE)GM.1943-5622.0000845.
- Terzaghi, K. 1943. *Theoretical soil mechanics*, New York, John Wiley.
- Topp, G.C. 1969. Soil-water hysteresis measured in a sandy loam compared with the hysteretic domain model. *Soil Science Society of America Journal* 33: 645-651.
- Wong, T.T., Fredlund, D.G. & Krahn, J. 1998. A numerical study of coupled consolidation in unsaturated soils. *Canadian Geotechnical Journal* 35: 926-937.
- Zhou, A.N., Sheng, D. & Carter, J. P. 2012. Modelling the effect of initial density on soil-water characteristic curves. *Géotechnique* 62(8): 669-680.
- Zhou, W.H., Zhao, L.S. & Li, X.B. 2014. A simple analytical solution to one-dimensional consolidation for unsaturated soils. *International Journal for Numerical and Analytical Methods in Geomechanics* 38: 794-810.